
EXPERIMENTAL DISTRIBUTED NETWORK OF VLF RECEIVERS FOR THUNDERSTORM ACTIVITY MONITORING IN THE BAIKAL NATURAL TERRITORY

I.D. Tkachev

*Institute of Solar-Terrestrial Physics SB RAS,
Irkutsk, Russia, tid007@iszf.irk.ru*

R.V. Vasilyev

*Institute of Solar-Terrestrial Physics SB RAS,
Irkutsk, Russia, roman_vasilyev@iszf.irk.ru*

O.S. Zorkaltseva

*Institute of Solar-Terrestrial Physics SB RAS,
Irkutsk, Russia, meteorologistka@gmail.com*

A.S. Poletaev

*Irkutsk National Research Technical University,
Irkutsk, Russia, poletaevas@ex.istu.edu*

A.G. Chensky

*Irkutsk National Research Technical University,
Irkutsk, Russia, zavmts@ex.istu.edu*

K.M. Vasiliev

*Institute of Solar-Terrestrial Physics SB RAS,
Irkutsk, Russia, vasilievm@iszf.irk.ru*

R.R. Salimgoreev

*Irkutsk State University,
Irkutsk, Russia, salimgoreev.renat@gmail.com*

Abstract. The paper describes the current state of the lightning location network deployed in the Irkutsk Region and the Republic of Buryatia, which includes four stations. It is based on the results obtained during several stages of the project “Fundamental principles, methods, and technologies for digital monitoring and forecasting of environmental situation of the Baikal Natural Territory”. We present a diagram of the VLF receiver in use. Data processing, features of some algorithms, and the rationale for their choice are described in detail. Developing processing algorithms and further

upgrading them have provided lightning discharge maps with a period of several minutes. We present intermediate results of the network operation, a lightning discharge distribution map and give recommendations for further developing and upgrading the lightning location network.

Keywords: lightning location networks, VLF receiver, lightning discharges, atmospheric electricity, thunderstorm activity monitoring.

INTRODUCTION

One of the most effective ways to monitor thunderstorm activity is networks of very low-frequency (VLF) radio receivers, which are synchronized by a single time standard and record pulse signals from lightning discharges. Lightning location networks (LLN) can be divided into global and regional by the coverage area. Global ground-based networks include WWLLN [Lay et al., 2004], NLDN [Cummins et al., 1998], NALDN [Orville et al., 2002], GLD360 [Naccarato et al., 2010], the worldwide non-commercial lightning detection and location network Blitzortung [<https://www.blitzortung.org/>], BLNET [Qie et al., 2020], etc. With advances in technology and active exploration of near-Earth space, another method of detecting lightning discharges has emerged: installation of Lightning Imaging Sensors (LIS) on board spacecraft with different orbits. For example, one of these devices is placed on ISS [Zhang et al., 2023]. Basically, the equipment for optical localization of lightning discharges is installed on board geostationary meteorological satellites [Chen et al., 2021; <https://www.eumetsat.int/features/animations-europes-first-lightning-imager>].

On the territory of the Russian Federation, a network covering most of the country can be considered global.

Currently, this category may include several LLNs differing in parameters and tasks: LLN ALWES [<http://www.alwes.ru>], LLN SRC Planet, the High-Mountain Geophysical Institute (HMGI) [Gorlova, 2020], LLN Roshydromet based on Alwes sensors. Until 2019, LLN Vereya-MR monitored thunderstorm activity throughout the Russian Federation [Moskovenko et al., 2012]. Servicing a large number of receivers spread over an extended territory requires a large amount of financial and human resources. Thunderstorm activity is therefore often studied using regional LLNs. The main advantage of regional LLNs is the accuracy of determining the location of a lightning discharge. It can be as high as tens and hundreds of meters. Noteworthy among regional LLNs in the Russian Federation are NNLDN [Sarafanov et al., 2024], a Vaisala lightning recorder LS8000 operating in the North Caucasus since 2008 [Adzhiev et al., 2013], single-point and multi-point monitoring systems in Yakutia [Kozlov et al., 2023; Tarabukina, Kozlov, 2018], as well as various local LLNs based on Alwes sensors involved in oil and gas industry in the Russian Federation. There are studies in which thunderstorm activity in the region is analyzed using sensor data from foreign networks WWLLN and Blitzortung [Karanina et al., 2017; Nechepurenko et al., 2022; Selivanov et al., 2022].

The Institute of Solar-Terrestrial Physics of the Siberian Branch of the Russian Academy of Sciences (ISTP SB RAS) supported the work of one of the Vereya-MR LLN stations from 2012 to 2018. During this period, a database of lightning discharges was created, and it was used for cluster analysis of lightning discharges in order to estimate key parameters of thunder cells [Tkachev et al., 2021]. The joint temporal dynamics of thunderstorms and forest fires has also been examined [Vasilyev et al., 2023]. In 2019, Vereya-MR ceased to exist, hence the need to establish a network of receivers in the Baikal Natural Territory to monitor thunderstorm activity and conduct further research.

In 2020–2023, under the project "Fundamental principles, methods, and technologies of digital monitoring and forecasting of the environmental situation of the Baikal Natural Territory" [Bychkov et al., 2022], ISTP SB RAS and Irkutsk National Research Technical University (INRTU) deployed a new LLN in the Irkutsk Region and the Republic of Buryatia. Analysis of thunderstorm activity based on Vereya-MR data and information from [Filippov, 1974] helped to find regions of the Baikal Natural Territory with the maximum number of thunderstorms. Stations of the new LLN were placed according to the data. To date, four recording stations have been put into operation.

When creating network elements, we developed VLF

receivers, algorithms for obtaining and collecting VLF radio broadcast data, and algorithms for secondary data processing: searching for lightning pulses and determining lightning discharge coordinates. Test operation of the network made it possible to perform primary analysis of thunderstorms, recorded in the summer of 2022, to improve secondary processing algorithms, to specify the location of additional stations of the network, and to evaluate its effectiveness. The research results have determined further stages of thunderstorm activity monitoring in the Baikal Natural Territory and the possibility of using the network's data for protecting infrastructure and for forest protection measures.

We describe the structure of the network and algorithms of its operation, as well as compare data on lightning discharges and clouds obtained during the test operation.

1. STRUCTURE OF THE LIGHTNING LOCATION NETWORK

VLF receiver

A recorder of the lightning location network is a VLF/LF digital radio receiver developed from a software-defined radio (SDR) [Dillinger et al., 2003]. Its general schematic diagram is given in Figure 1, *a*.

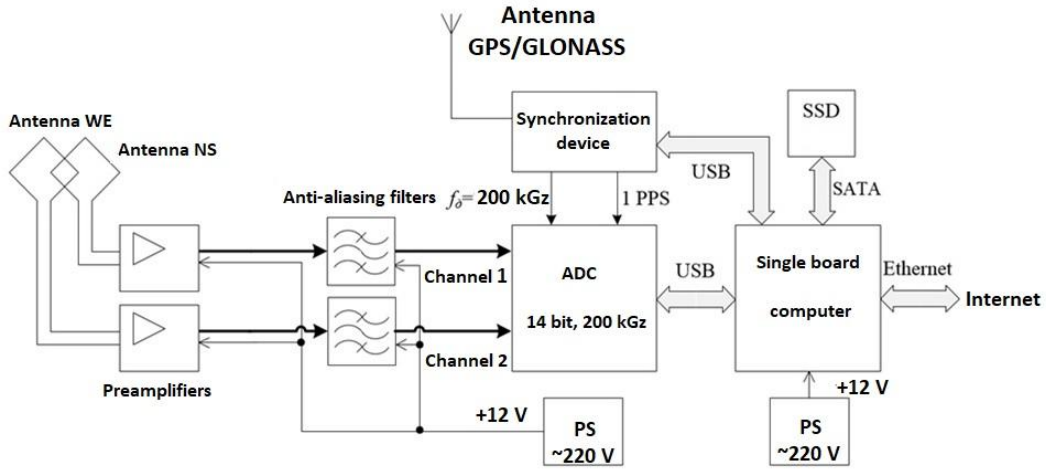


Figure 1. Schematic diagram of the lightning location network's recorder (*a*); a set of equipment for one of the stations (*b*)

Lightning discharges are the main source of electromagnetic emission of natural origin. The pulse energy is distributed in a relatively wide frequency range, but it largely falls on frequencies below 100 kHz with maximum emission in the 1–10 kHz frequency range [Uman, 1987]. Radio waves are received by orthogonal multiturn loop antennas. Wide-frequency-range preamplifiers, located in the immediate vicinity of them, coordinate the receiver's linear path with the antenna. The amplifier is based on an ultra-low-noise chip KR538UN3A, designed for low-resistance inductive sensors. Antialiasing filters limit the emission spectrum by suppressing fluctuations at frequencies below 1 kHz and above 50 kHz. ADC L-card E14-140 is used for data acquisition. The ADC conversion frequency is 200 kHz with two-channel reception (100 kHz per channel). The ADC capacity is 14 bits, with a dynamic range ± 2.5 V, quantization step $\Delta = 5/2^{14} = 0.305$ mV. The ADC unit supports regimes of external synchronization of data conversion and acquisition start. The synchronization device provides data timing to UTC, using the GPS/GLONASS unit Ublox M8T. Data processing is implemented in software by a single-board computer.

Layout of the equipment set is shown in Figure 1, *b*. It includes two circular loop antennas, two preamplifiers in shielded moisture-proof sides, two connecting cables KVK 2P 2×0.52 20 m long, a linear receiver unit, a GPS/GLONASS antenna, a single-board minicomputer, a keyboard, a mouse, switched and linear power supplies.

Data Acquisition Program

The recorder control program (Figure 2) starts automatically when power is applied. After startup, the exe-

cutable downloads saved settings from a file and puts the system into the sleep mode for GPS/GLONASS synchronization pulses. Data acquisition is started at the hardware level upon arrival of the 1PPS pulse. Data is extracted from the buffer in samples per 1 s (200000 readings, 100000 for each channel). The view window operates in the oscilloscope or spectrum analyzer mode. After each 1PPS pulse arrives, the program receives an NMEA packet with time and coordinate data. If there is no navigation data for 30 s, data acquisition stops and starts again. Files are saved in 1 min samples. The raw data sample is a set of binary files obtained with ADC settings: 200 kHz, 1 channel, 14 bits, ± 2.5 V.

Location of receiving stations

Recording stations of the lightning location network are placed on the territory of ISTP SB RAS observatories and units of aviation forest protection of the Baikal Natural Territory. Coordinates of the stations: Tory village — 51.8109° N, 103.0775° E; Listvyanka village — 51.8463° N, 104.8927° E; Bratsk — 56.315° N, 101.7555° E; Nizhneangarsk village — 55.7932° N, 109.580° E (Figure 3, *d*). Panels *a–c* exhibit images of antennas of lightning location stations and equipment of the recording complex of one of the stations. In addition to these four stations, there are two equipment sets for the planned expansion of the coverage area of the lightning location network and for immediate replacement of equipment in case of failure of one of the stations.

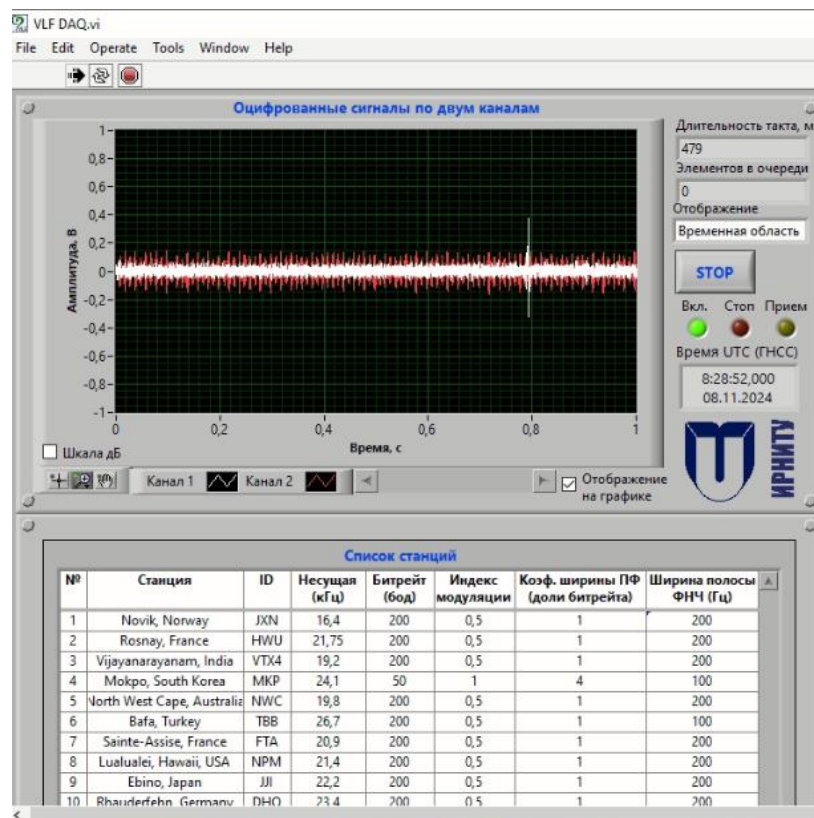


Figure 2. Data acquisition program panel

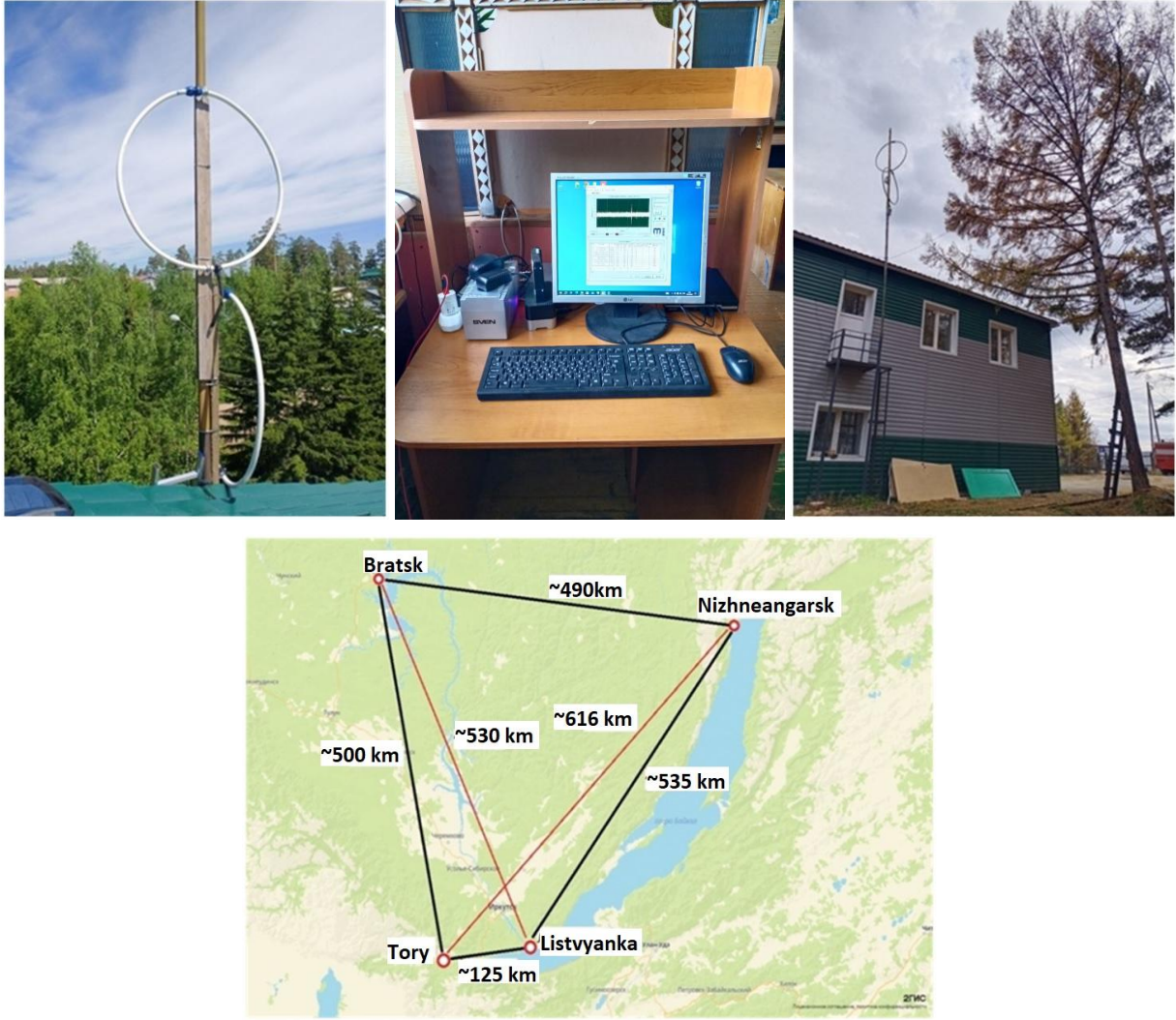


Figure 3. Installed antennas of the lightning location station in Bratsk (a); work station of the lightning location network (b); installed antennas of the lightning location station in Nizhneangarsk village (c); lightning location stations in the Irkutsk Region and the Republic of Buryatia as of October 2024 (d)

2. DATA PROCESSING ALGORITHMS

Data processing in the lightning location network is divided into several stages. Since the amount of raw data takes up a lot of space on the hard disk (~30 GB per day), it is advisable to isolate signals from lightning discharges and save small time scans (~6 μ s) associated with this discharge. An automatic algorithm is therefore started at each individual recording station, which extracts pulses from the total data array whose amplitude exceeds the preset threshold, and there are more than three significant points (pulse-associated points exceeding the threshold amplitude). Thus, the following parameters are tabulated: pulse recording time (defined as the time of maximum pulse amplitude), power (amplitude), duration, and the direction from which the pulse was recorded (azimuth). Figure 4 exemplifies the recorded pulse.

The generated table with the parameters of recorded pulses is transmitted to the server. After that, it is necessary to establish a correspondence between the pulses recorded at different stations and their driven lightning

discharges. Given the distance between the stations and the speed of light, the maximum allowable time difference Δt_{\max} between pulses is calculated for all possible pairs of stations. In the first version of the algorithm, the search was made as follows: the pulse time recorded at the first station was selected, and this time was subtracted from times of all pulses recorded at the second station. The data sets obtained at the first and third stations are compared in a similar way. Next, such time differences (Δt_{1-2} , Δt_{1-3} , Δt_{2-3}) were selected whose moduli did not exceed the maximum allowable value (Δt_{\max}) for the chosen pair of stations. The pulse times were tabulated. A limitation of this algorithm is the need to compare the time of one pulse with the times of all pulses from other stations (there may be more than 100000) at each iteration of the cycle, which, in turn, greatly slows down data processing.

A new algorithm was therefore implemented. It consists of the following: the time is selected at the first station and a comparison cycle is initiated with times from the second station. Once $\Delta t_{1-2} > \Delta t_{1-2\max}$, the comparison stops, the pulse time from the second station is fixed which fulfils the condition (if it exists), then the algorithm switches to

comparing with pulse times from other stations in view of the above condition. At the same time, the pulse time index is stored at which the condition $-\Delta t_{1-2\max} < \Delta t_{1-2}$, etc., begins to hold. This action at the next iteration of the cycle allows us to start comparing not with the beginning of the list of times from another station, but with a certain index of the list. Thus, a sliding window is implemented for which the condition $-\Delta t_{\max} < \Delta t < \Delta t_{\max}$ is met. This approach in the pulse search algorithm makes it possible to speed up data processing tenfold compared to its previous version. Recording of the same discharge by two stations is exemplified in Figure 5.

At the stage of determining whether the pulses recorded by different stations belong to the same lightning discharge, it is important to monitor time synchronization between the stations. At each station, it occurs with the aid of a GNSS unit that receives a corrective PPS

signal from a satellite. However, laboratory experiments have found that sometimes there may be an incorrect timing of a PPS signal, which causes a time shift. This may occur when the satellite signal reception gets worse or there are not enough visible satellites. An additional tool for monitoring and correcting the time at the stations has therefore been developed. Since the trace program records minute files, the pulse times are compared between all pairs of stations for the same minutes. The pulse time from the first station is selected and subtracted from the pulse times obtained by the second station; the difference is stored in an array. At the next step of the cycle, the second pulse from the first station is selected and also subtracted from all pulses at the second station,

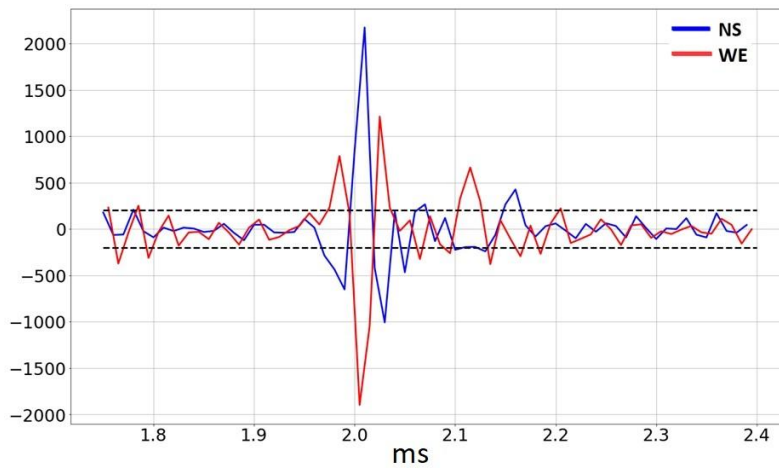


Figure 4. A lightning discharge pulse. Data from two channels: north—south (blue curve), west—east (red curve). The dashed line is the threshold amplitude from which the pulse is identified. Along the horizontal axis is the time scan of one pulse (μ s); along the vertical axis is the pulse amplitude in relative units.

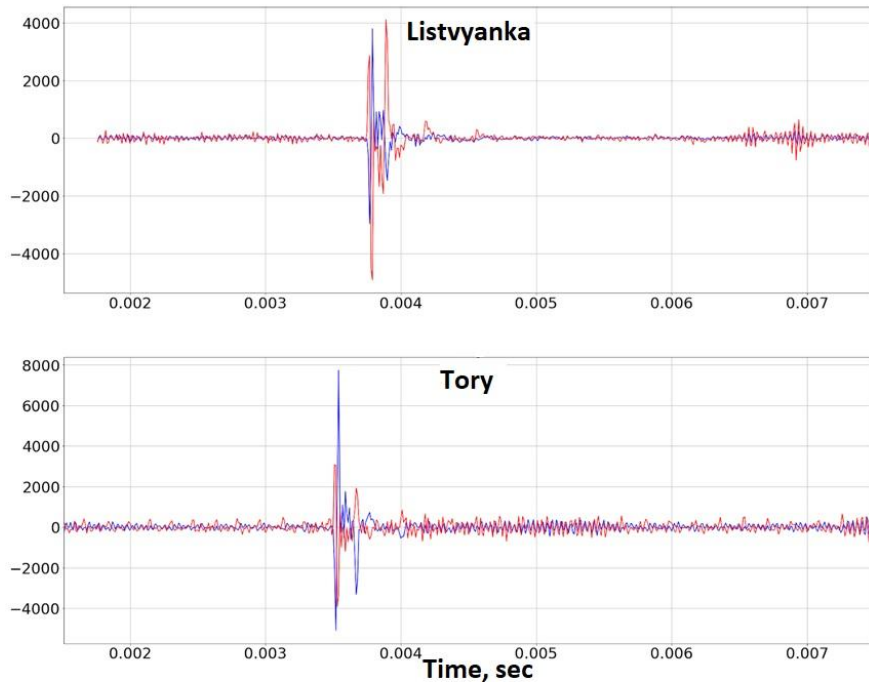


Figure 5. Recording of the same atmospheric at two stations: *a* — a pulse recorded at the station Listvyanka; *b* — at the station Tory. Along the vertical axis is the amplitude (relative units)

which were recorded during that minute. Next, a minute-by-minute histogram of time differences is constructed for any two stations (Figure 6).

If there is no time shift between the stations, the pulses that belong to the same lightning discharges will be located in the range of time differences limited to the distances between the stations (Figure 6, *b*). For example, the distance between Tory and Listvyanka is ~ 130 km, the maximum time difference between the recorded pulses at these stations, in order to consider these pulses as belonging to the same lightning discharge, should be no more than ~ 430 μ s. If we have a time shift (Figure 6, *a*), we can see a pulse cluster shift on this time difference map. Using time maps for several stations, we can determine at which of the stations and by what amount the time shift occurs in order to further level this shift manually. After table with the sorted pulses is formed, the stage of recovering lightning discharge coordinates begins.

Recovery can take place under different scenarios depending on the number of operating stations at a given time. When using one or two stations for lightning location, it is advisable to apply the amplitude-phase method [Kozlov et al., 2010; Kononov et al., 1986]. Two loop antennas (in the above implementation of the circle-shaped VLF receiver), arranged orthogonally in the north—south and west—east directions respectively, allow

us to find the direction (azimuth), from which the electromagnetic wave arrived, from signal phase (Figure 7, *a*).

In this case, the pulse amplitude $A(r)$, represented as a function of the pulse amplitude dependence on the distance to a discharge, allows us to estimate the range of lightning. Thus, by combining two signal parameters (amplitude, azimuth), it is possible to determine lightning discharge coordinates, using one lightning location station. Yet, this method has drawbacks; one of them is the low accuracy of positioning.

If we know the signal delay time relative to each recording station and directions (azimuths) along which the pulse arrived, we can determine geo-position of the lightning discharge in the operating conditions of two lightning location stations. Figure 7, *b*, by the example of two stations (Tory, Listvyanka), illustrates the determination of discharge geo-position by the hyperbolic azimuthal method [Kononov et al., 1986]. The time delay of the signal and the distance between the stations allow us to construct a hyperbola on which there may be possible lightning discharge coordinates. Using azimuths of the recorded electromagnetic pulse, we can draw the direction to each station. Intersection of the lines and the hyperbola yields an area in which, with some error, lightning discharge coordinates can be found.

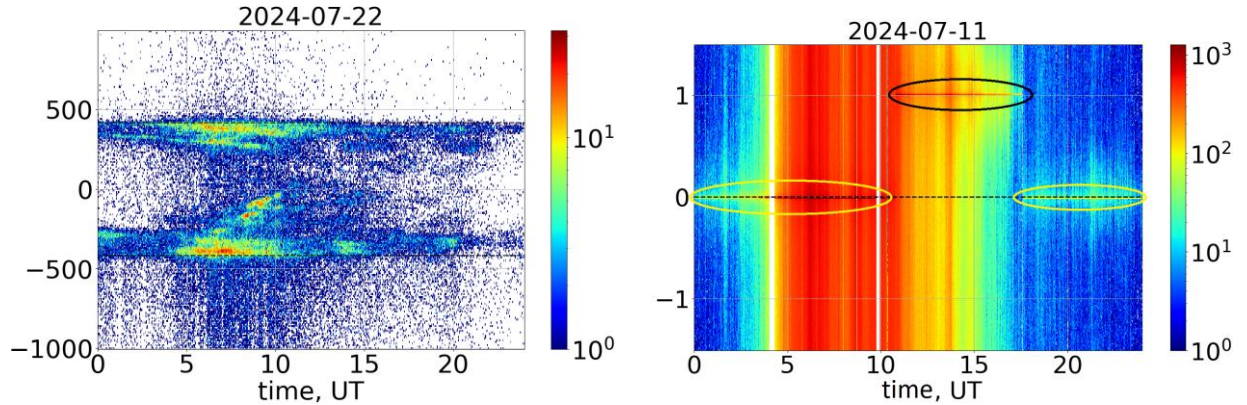


Figure 6. Time difference map to control the time shift between stations for Tory—Listvyanka: *a* — without a time shift (on the vertical axis, time in μ s); *b* is a time shift at one of the stations (on the vertical axis, time in seconds). Yellow ellipses indicate time points without shift; the black ellipse marks the time interval when an incorrect PPS timing occurred at one of the stations.

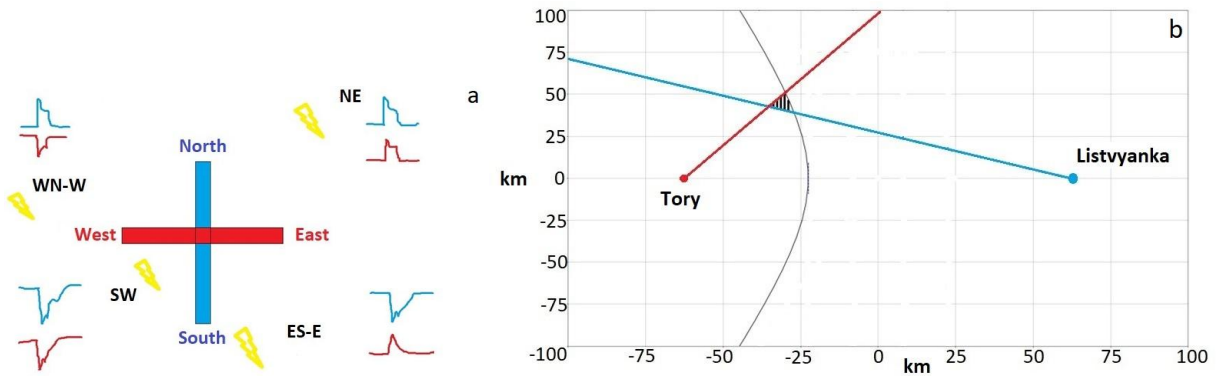


Figure 7. Schematic example of determining the azimuth of a recorded pulse, using two loop orthogonal antennas (*a*). The color indicates antenna directions and their associated conventional forms of received signals. Determination of the location of a discharge by the hyperbolic azimuthal method, using two stations as an example (*b*). The red dot is the station in Tory; the blue dot is the station in Listvyanka; the shaded area is the possible location of the lightning discharge.

Three or more recording stations make it possible to employ the Time Difference of Arrival (TDoA) method [Proctor, 1971] to find lightning discharge coordinates from the difference between pulse recording times at the stations. If lightning location stations are spaced apart when the sphericity of Earth has a significant effect on electromagnetic wave propagation (distances around >1000 km), as, for example, in WWLLN, the Time of Group Arrival (TOGA) method should be applied [Dowden et al., 2002]. The stations in the network considered are ~500 km apart, so the TDoA method is used in processing. This paper presents data for 2023 when three recording stations were operating. Data processing and analysis were carried out by adapting the algorithm for analytical solution of the system of hyperbolic equations described in [Takagi et al., 2022]. It is based on the TDoA method. To calculate lightning discharge coordinates, it is enough to know the difference between electromagnetic pulse recording times at three stations (minimum) and coordinates of the corresponding stations:

$$\sqrt{(x-x_1)^2 + (y-y_1)^2} - \sqrt{(x-x_2)^2 + (y-y_2)^2} = R_{12}, \quad (1)$$

$$\sqrt{(x-x_1)^2 + (y-y_1)^2} - \sqrt{(x-x_3)^2 + (y-y_3)^2} = R_{13}, \quad (2)$$

$$\sqrt{(x-x_2)^2 + (y-y_2)^2} - \sqrt{(x-x_3)^2 + (y-y_3)^2} = R_{23}, \quad (3)$$

$$R_{12} = c(t_2 - t_1), \quad (4)$$

$$R_{13} = c(t_3 - t_1), \quad (5)$$

$$R_{23} = c(t_3 - t_2), \quad (6)$$

where (x_1, y_1) , (x_2, y_2) , (x_3, y_3) are the coordinates of the corresponding recording stations; (x, y) are the coordinates of the desired lightning discharge; t_1, t_2, t_3 are the pulse recording time at the corresponding station; c is the speed of light. Solving analytically system of equations (1)–(3), we obtain a point that is the center of mass of the region formed by intersection of three hyperbolas (Figure 8). Thus, the described algorithm yields lightning discharge coordinates.

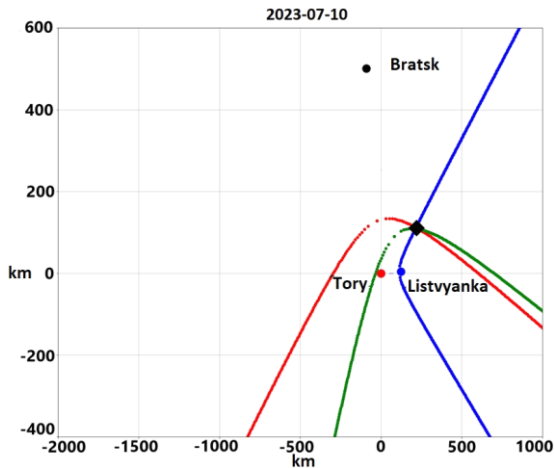


Figure 8. Visualization of TDoA solution for finding a lightning discharge coordinate. Colored dots represent the recording stations: black — Bratsk, red — Tory, blue — Listvyanka; black rhombus marks the intersection of hyperbolas

3. RESULTS AND DISCUSSION

The system was put into operation in several stages. In the summer of 2022, two stations were commissioned near Tory and Listvyanka villages. Due to the data obtained, processing algorithms were adjusted, improved, and performance of time synchronization of the recording stations was assessed. The lightning discharge coordinates were recovered by the hyperbolic azimuthal method. In 2023, another recording station was put into operation in Bratsk. This made it possible to implement the algorithm for recovering lightning discharge coordinates by the TDoA method, which increased the accuracy of finding lightning coordinates.

Information from the described lightning location network can be compared with satellite cloud data to assess the validity of the information (Figure 9). Cloud maps were obtained using data from NOAA satellites 18 and 19. Dates in Figure 9 correspond to the time of the satellite image.

Blue dots denote lightning discharges accumulated within ± 30 min from the time of the image. The diameter of the blue dot depends on the discharge power. The images show the presence of cloud fields that coincide closely with the location of lightning discharges. Such regions are generally located inside the Bratsk—Tory—Listvyanka triangle. At the same time, there are places with lightning discharges, but without clouds. This may be due to the choice of a large interval of accumulation of lightning discharges during which the location of the clouds could change. Moreover, the resulting maps show a structured pattern of lightning discharges in the form of parallel lines or diverging rays. To explain these features, we have simulated the operation of the lightning location network.

A 1000×1000 km section of Earth's surface containing stations of the lightning location network was represented as a plane square coordinate grid with a step of 10 km. For this area, we calculated the time it took a lightning discharge signal to propagate from each node of the coordinate grid to each of the three recording stations. The obtained time intervals were rounded depending on the time resolution of ADC (10 μ s), and then they were used to recover coordinates of the grid nodes in accordance with system of equations (1)–(6). The results of this simulation are presented in Figure 10.

Green dots indicate coordinates such that system of equations (1)–(6) has a unique solution in the simulation. In other cases, two solutions suggest that three hyperbolas have two points of intersection at the same time and there is no single solution. Orange dots and empty areas in Figure 10 denote coordinates for which a correct solution cannot be chosen from two solutions or the algorithm cannot find any solution of (1)–(6) at all.

Furthermore, it is clearly seen that in areas, where branches of hyperbolas intersect at acute angles, the position of the intersection points differs significantly from the coordinates of a regular square grid. This is due to the fact that the 10 μ s time resolution for these geometric locations results in a significant distortion of the position of the recovered coordinates relative to the original ones. It is this situation that manifests itself in the features of the location of the real reconstructed lightning discharges in Figure 9.

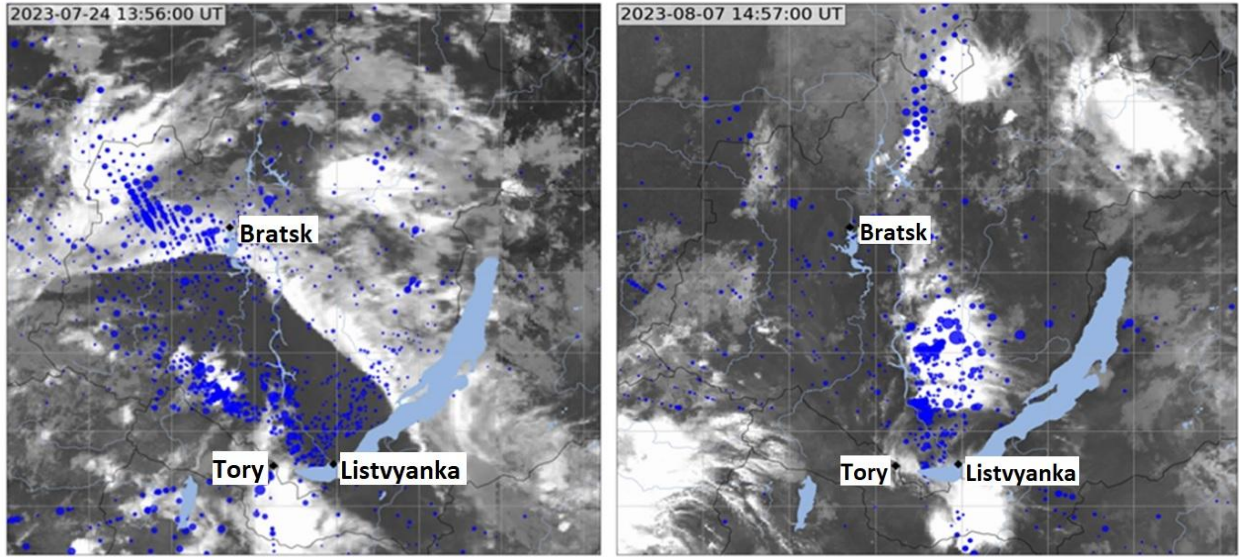


Figure 9. Comparison of the location of lightning discharges according to data from the lightning location network (blue dots) with cloudiness over the Irkutsk Region and the Republic of Buryatia observed by NOAA satellites 18 and 19. Dates of the images are shown at the top left

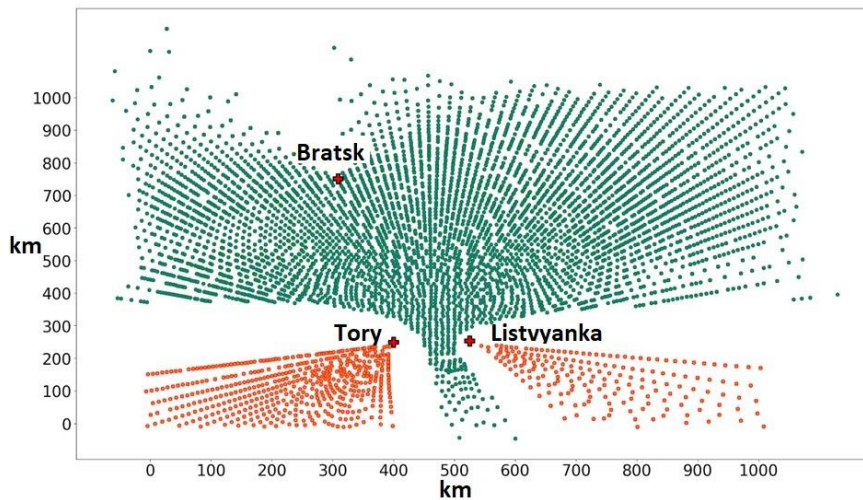


Figure 10. Map of simulation of recovery of lightning discharge coordinates by an algorithm based on the TDoA method for three stations. Green dots are areas where the algorithm gives one solution; orange dots, two solutions; however, with the aid of additional conditions we can choose an unambiguous coordinate. Red pluses mark lightning location stations the distances between which are calculated from their actual geographical locations.

Taking into account the described features of the system and the data processing algorithms, we have obtained statistics on the distribution of lightning discharges for the thunderstorm season (April–October) of 2023 (Figure 11). After completing all stages of adjustment, the three-station network has been fully operational since July.

It can be seen that the number of recorded discharges per season is, on average, ~25000 per day. Increased thunderstorm activity on July 16 stands out sharply against the background of average values, when more than 200000 discharges were recorded per day. The actual number of discharges per day may be slightly larger than the received maps show. This conclusion can be drawn because the total number of discharges per day at each station is different. This is due to the noise level at the recording stations,

and since the recording threshold is set experimentally and higher than noise during data processing, the number of pulses for further comparison may vary.

According to the Hydrometeorological Research Center of the Russian Federation (HRC), increased thunderstorm activity in the Irkutsk Region on July 16 was associated with a cyclone whose center was observed near Bratsk. The central and southern parts of the region were affected by the cyclone's warm sector. A high-altitude trough was recorded in the middle and upper atmosphere, which further increased convection in the afternoon. In Figure 12, red circles indicate the stations that recorded the thunderstorms. The center of thunderstorm activity is seen to be over the Irkutsk Region.

Daily variations in the number of lightning discharges were compared with the *CAPE* (Convective Available

Potential Energy) index (Figure 13), taken from the ERA5 reanalysis archive [Hersbach et al., 2020]. *CAPE* is a measure of the ability of the atmosphere to support the upward motion of air and represents the integrated amount of work that the upward (positive) buoyancy force will do over a unit of air mass if it rises vertically throughout the atmosphere. Positive *CAPE* values indicate that the air mass is warmer than its surroundings, i.e. convectively unstable. To *CAPE* from 0 to 1000 J/kg corresponds a slight instability of the atmosphere. At the same time, there may be light rainfall. At 1000–2500 J/kg, there is moderate instability with showers, thunderstorms, and squalls; at 2500–3500 J/kg, strong instability; at >3500 J/kg, severe

instability with strong and very strong thunderstorms, squalls, and hail. The values in Figure 13 were calculated for 50°–60° N and 95°–110° E respectively. For July 16, daily variation was plotted for average *CAPE* of the above region (red dashed curve), as well as for maximum *CAPE* (red solid curve). The variation for average *CAPE* follows the daily distribution of lightning discharges quite well. However, the maximum index value in this case only at 12:00 UT exceeds 1000 J/kg, which corresponds to moderate instability with showers, thunderstorms, and squalls.

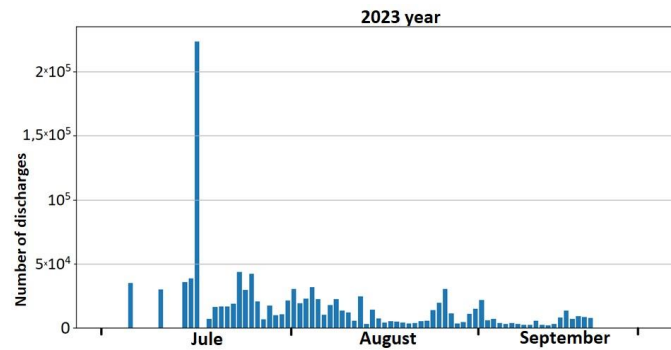


Figure 11. Lightning discharge distribution statistics for the thunderstorm season in 2023

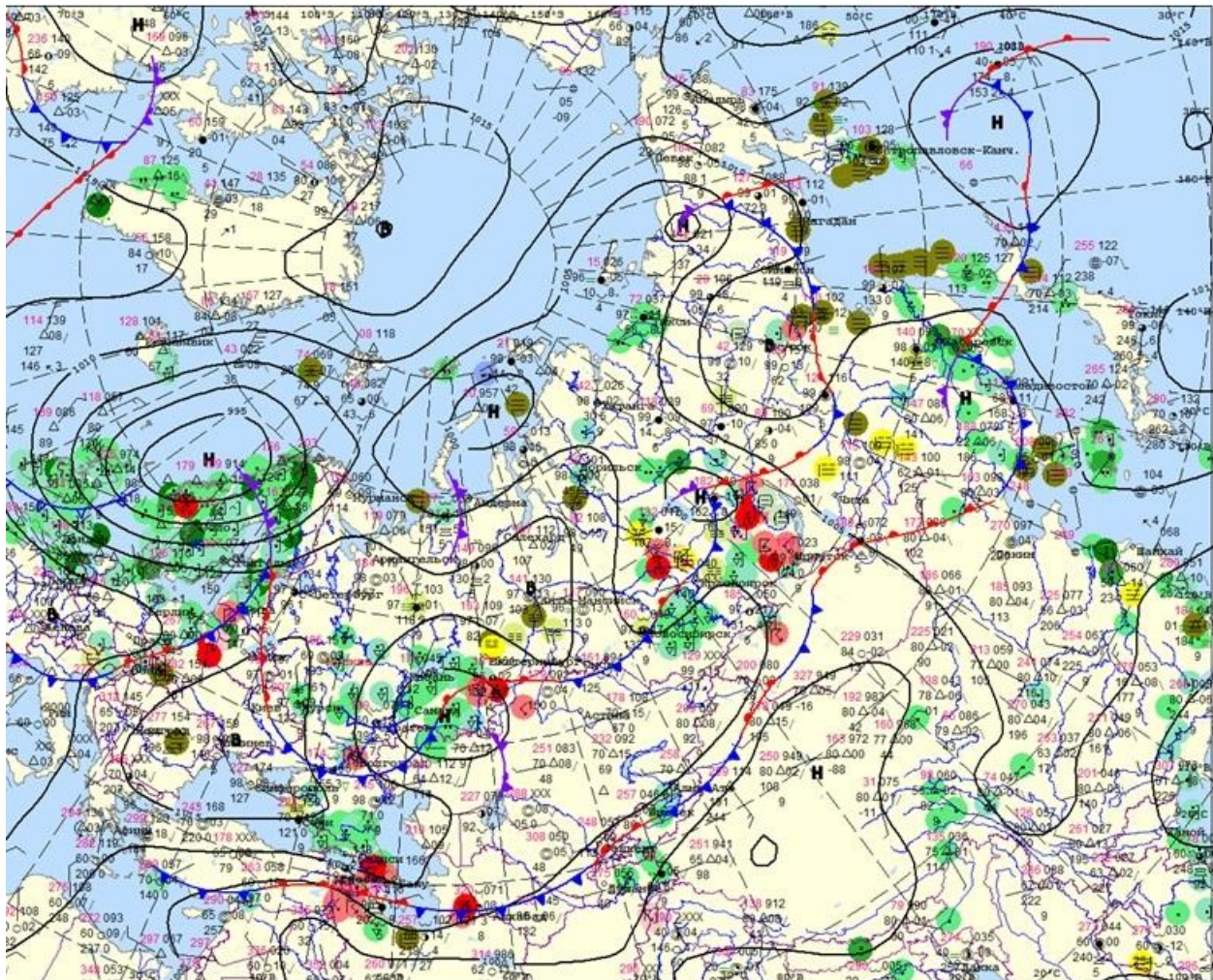


Figure 12. Synoptic surface map according to HRC data on July 16, 2023 at 18:00 UTC [<https://meteoinfo.ru/mapsynop>]

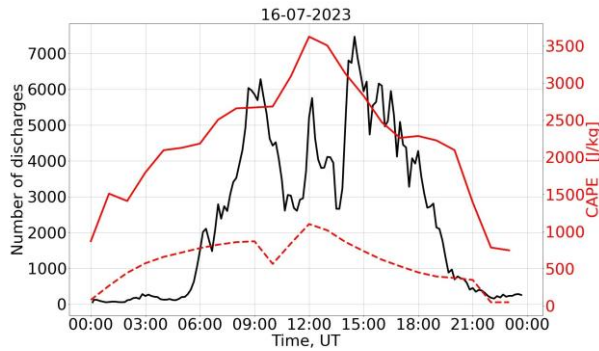


Figure 13. The black curve is the daily distribution of the number of lightning discharges for July 16, 2023; the red curve is a change in maximum CAPE; and the dashed red curve is a change in average CAPE for the same date.

This can be explained by the fact that $CAPE$ was averaged over a large area. In turn, for variations of maximum $CAPE$ there is a value above 3500 J/kg, which corresponds to a severe instability with strong and very strong thunderstorms. The maximum number of lightning discharges was recorded around 14:30 UT, and maximum $CAPE$ was still high and indicated the presence of strong convective instability. To study a more accurate relationship between the variation in the number of lightning discharges and $CAPE$, it is necessary to conduct an additional analysis of the spatial distribution of discharges.

Thus, the problem of recording regional thunderstorm activity at an acceptable level can be solved using a small network of VLF lightning direction finders consisting of orthogonal loop antennas for determining the azimuth of an electromagnetic signal from a lightning discharge and equipped with synchronization systems based on GNSS receivers. The location of lightning discharges recorded inside the triangle formed by the lightning location stations is recovered with acceptable accuracy by the proposed algorithms. This is confirmed by a close match between detected discharges and current cloud fields. A drawback can be considered to be cases in which algorithms ambiguously define the location of a discharge; therefore, the fourth recording station has been put into operation.

The distortions resulting from low time resolution can be eliminated by replacing ADC with faster ones or by trying to implement the procedure for re-digitizing the signal by interpolation methods. The device of the recording systems of the described lightning location network will allow for retrospective analysis of the accumulated information since during operation at each station a segment of the digital oscillogram of a recorded pulse from a lightning discharge is stored.

Despite some incompleteness of the network consisting of three lightning location stations, the information it provides is sufficient to examine the integral characteristics of the rate of lightning occurrence and variations in atmospheric parameters. The illustrative example of comparing the integral number of discharges with the statistical characteristics of the $CAPE$ index (see Figure 13) suggests that other integral parameters

of the atmosphere over a region covered by the lightning location network, which determine thunderstorm activity, or vice versa, are affected by it (chemical composition of small components, aerosol density, ion density, ionospheric plasma, etc.), can be studied in a similar way.

CONCLUSION

The main result of this work is the commissioning of an experimental lightning location network based on VLF receivers in the Irkutsk Region and the Republic of Buryatia. The development and assembly of the equipment, the realization of the algorithms for processing and interpreting the obtained data have been implemented by ISTP SB RAS and INRTU research teams. The developed VLF receivers of the network comply with the level of equipment used in Russia and abroad for recording lightning discharges.

The location of the stations of the network was chosen taking into account the analysis of thunderstorm activity in the Baikal Natural Territory and mathematical modeling of recovery of lightning discharge coordinates when the location of the recording stations changes.

We have examined in detail the methods and features of obtaining lightning discharge coordinates, using data from two and three lightning location stations. We have shown that the location of lightning discharges is restored with acceptable accuracy by the proposed algorithms if the recorded discharge occurs inside the triangle formed by the lightning location stations. At the same time, we observed cases of ambiguous determination of the discharge location by the algorithms; therefore, the fourth recording station has been put into operation. In the future, it is planned to expand the network to six stations in order to finally solve the problem of spatial uncertainty. The construction of maps with lightning discharge coordinates is the result of the work at the current stage.

Another task is to realize an automated processing providing lightning discharge maps with a period of several tens of minutes. The in-situ results have shown that the developed software can implement the process of obtaining lightning discharge maps every 10–15 min. Thus, in addition to retrospective data processing and solving scientific problems, it will be possible to use data from the described lightning location network as an additional tool for near-real-time monitoring of thunderstorm activity in the region.

The work was financially supported of the Ministry of Science and Higher Education of the Russian Federation (Subsidy No. 075-GZ/C3569/278).

REFERENCES

- Adzhiev A.Kh., Stasenkov V.N., Tapashkanov V.O. Lightning detection system in the North Caucasus. *Meteorologiya i gidrologiya* [Meteorology and Hydrology]. 2013, no. 1, pp. 2–11. (In Russian).
- Bychkov I.V., Gladkochub D.P., Ruzhnikov G.M. *Fundamental principles, methods and technologies of digital monitoring and forecasting of the environmental situation in the Baikal natural territory*. Russian Academy of Sciences. Siberian Branch. Matrosov Institute of System Dynamics

- and Control Theory. Integration projects of SB RAS. Novosibirsk, 2022, vol. 48, 345 p. DOI: [10.53954/9785604788943](https://doi.org/10.53954/9785604788943). (In Russian).
- Chen Z., Qie X., Sun J., Xiao X., Zhang Y., Cao D., Yang J. Evaluation of Fengyun-4A Lightning Mapping Imager (LMI) performance during multiple convective episodes over Beijing. *Remote Sens.* 2021, vol. 13, no. 9, 1746. DOI: [10.3390/rs13091746](https://doi.org/10.3390/rs13091746).
- Cummins K.L., Krider E.P., Malone M.D. The US National Lightning Detection Network TM and applications of cloud-to-ground lightning data by electric power utilities. *IEEE Transactions Electromagnetic Compatibility.* 1998, vol. 40, no. 4, pp. 465–480. DOI: [10.1109/15.736207](https://doi.org/10.1109/15.736207).
- Dillinger M., Madani K., Alonistioti N. Software defined radio: architectures, systems, and functions. *Wiley.* 2003, 454 p.
- Dowden R.L., Brundell J.B., Rodger C.J. VLF lightning location by time of group arrival (TOGA) at multiple sites. *J. Atmos. Solar-Terr. Phys.* 2002, vol. 64, no. 7, pp. 817–830. DOI: [10.1016/S1364-6826\(02\)00085-8](https://doi.org/10.1016/S1364-6826(02)00085-8).
- Filippov A.Kh. *Grozy Vostochnoj Sibiri* [Thunderstorms in Eastern Siberia]. Leningrad, Hydrometeoizdat Publ., 1974, 75 p. (In Russian).
- Gorlova I.D. Study of thunderstorm activity by means of space and ground-based means. *Problems of military applied geophysics and monitoring of the state of the natural environment: Proc. VI All-Russian Scientific Conference.* St. Petersburg: A.F. Mozhaisky Military Space Academy, 2020, pp. 211–213. (In Russian).
- Hersbach H., Bell B., Berrisford P., Hirahara S., Horányi A., Muñoz-Sabater J., Nicolas J., et al. The ERA5 global reanalysis. *Quarterly J. Royal Meteorological Soc.* 2020, vol. 146, pp. 1999–2049. DOI: [10.1002/qj.3803](https://doi.org/10.1002/qj.3803).
- Karanina S.Yu., Kocheeva N.A., Karanin A.V. Spatial and temporal distribution of lightning discharges on the territory of the Altai-Sayan region. *Izvestiya vysshikh uchebnykh zavedenii. Severo-Kavkazskii region. Estestvennye nauki* [News of Higher Educational Institutions. North Caucasian Region. Natural Sciences], 2017, no. 4-1 (196), pp. 128–138. DOI: [10.23683/0321-3005-2017-4-1-128-138](https://doi.org/10.23683/0321-3005-2017-4-1-128-138). (In Russian).
- Kononov I.I., Petrenko I.A., Snegurov V.S. *Radiotekhnicheskie metody mestoopredeleniya grozovykh ochagov* [Radio-technical Methods for Locating Thunderstorm Centers]. Leningrad, Hydrometeoizdat Publ., 1986, 220 p. (In Russian).
- Kozlov V.I., Markova A.Yu., Shabaganova S.N. Errors in methods of observing lightning discharges using one- and two-point lightning detection systems. *Nauka i obrazovanie* [Science and Education], 2010, no. 1, pp. 7–12. (In Russian).
- Kozlov V.I., Tarabukina L.D., Vasiliev A.A. Development of lightning detection system in Yakutia. *Materialy IX Vserossiiskoi nauchnoi konferencii po atmosfernomu elektrichestvu: Voенно-kosmicheskaya akademiya imeni A.F. Mozhajskogo. Sankt-Peterburg* [Proc. IX All-Russian Scientific Conference on Atmospheric Electricity: A.F. Mozhaisky Military Space Academy. St. Petersburg]. 2023, pp. 278–287. (In Russian).
- Lay E.H., Holzworth R.H., Rodger C.J., Thomas J.N., Pinto O.Jr., Dowden R.L. WWLL global lightning detection system: Regional validation study in Brazil. *Geophys. Res. Lett.* 2004, vol. 31, L03102. DOI: [10.1029/2003GL018882](https://doi.org/10.1029/2003GL018882).
- Moskovenko V.M., Znamenshnikov B.P., Zolotarev S.V. Application of the Vereya-MR lightning-direction finding system in the interests of the Russian electric power industry. *Novoe v rossiiskoi elektroenergetike* [New in the Russian Power Industry], 2012, no. 2, pp. 15–23. (In Russian).
- Naccarato K.P., Pinto O.Jr., Garcia S.A.M., Murphy J.M., Demetriades N.W.S., Cramer J.A. Validation of the new GLD360 dataset in Brazil: First results. *Preprints. International Lightning Detection Conference.* Vaisala. 2010, pp. 1–6.
- Nechepurenko O.E., Gorbatenko V.P., Pustovalov K.N., Gromova A.V. Thunderstorm activity over Western Siberia. *Geosfernye issledovaniya* [Geospheric Research], 2022, no. 4, pp. 123–134. DOI: [10.17223/25421379/25/8](https://doi.org/10.17223/25421379/25/8). (In Russian).
- Orville R.E., Huffines G.R., Burrows W.R., Holle R.L., Cummins K.L. The North American Lightning Detection Network (NALDN) — First results: 1998–2000. *Monthly Weather Review.* 2002, vol. 130, no. 8, pp. 2098–2109. DOI: [10.1175/1520-0493\(2002\)130<2098:TNALDN>2.0.CO;2](https://doi.org/10.1175/1520-0493(2002)130<2098:TNALDN>2.0.CO;2).
- Proctor D.E. A hyperbolic system for obtaining VHF radio pictures of lightning. *J. Geophys. Res.* 1971, vol. 76, no. 6, pp. 1478–1489. DOI: [10.1029/JC076i006p01478](https://doi.org/10.1029/JC076i006p01478).
- Qie X., Yuan S., Chen Z., Wang D., Liu D., Sun M., et al. Understanding the dynamical-microphysical-electrical processes associated with severe thunderstorms 535 over the Beijing metropolitan region. *Science China Earth Sciences.* 2020, vol. 64, pp. 10–26. DOI: [10.1007/s11430-020-9656-8](https://doi.org/10.1007/s11430-020-9656-8).
- Sarafanov F.G., Shatalina M.V., Shlyugaev Yu.V., Mareev E.A. Modern lightning detection systems: global and regional aspects. *Fundamentalnaya i prikladnaya klimatologiya* [Fundamental and Applied Climatology]. 2024, vol. 10, no. 1, pp. 76–92. DOI: [10.21513/2410-8758-2024-1-76-92](https://doi.org/10.21513/2410-8758-2024-1-76-92). (In Russian).
- Selivanov V.N., Burtsev A.V., Ivonin V.N., Kolobov V.V. Analysis of lightning activity in the Murmansk region in 2021. *Trudy Kolskogo nauchnogo centra RAN. Seriya: Tekhnicheskienauki* [Proc. of the Kola Science Center of the Russian Academy of Sciences. Series: Technical Sciences]. 2022, vol. 13, no. 3, pp. 59–67. DOI: [10.37614/2949-1215.2022.13.3.006](https://doi.org/10.37614/2949-1215.2022.13.3.006). (In Russian).
- Takagi J., Kanazawa H., Ichikawa K., Mitamura H. A simple intuitive method for seeking intersections of hyperbolas for acoustic positioning biotelemetry. *PLOS One.* 2022, vol. 17, no. 11, e0276289. DOI: [10.1371/journal.pone.0276289](https://doi.org/10.1371/journal.pone.0276289).
- Tarabukina L.D., Kozlov V.I. Comparison of measurements of several lightning radio pulse recording systems. *Vestnik SVFU* [Vestnik of NEFU], 2018, vol. 64, no. 2, pp. 77–86. (In Russian).
- Tkachev I.D., Vasilyev R.V., Belousova E.P. Cluster analysis of lightning discharges: Based on Vereya-MR network data. *Solar-Terrestrial Physics.* 2021, vol. 7, iss. 4, pp. 85–92. DOI: [10.12737/stp-74202109](https://doi.org/10.12737/stp-74202109).
- Uman M.A. *The Lightning Discharge*. International Geophysics Series. Orlando: Academic Press. 1987, vol. 39, 390 p.
- Vasilyev R.V., Tashchilin M.A., Tatarnikov A.V. Comparison of the dynamics of thermal points and registered forest fires with the dynamics of lightning discharges in the Baikal natural territory. *Vychislitel'nyetekhnologii* [Computingtechnologies]. 2023, vol. 28, no. 6, pp. 37–45. DOI: [10.25743/ICT.2023.28.6.004](https://doi.org/10.25743/ICT.2023.28.6.004). (In Russian).
- Zhang D., Cummins K.L., Lang T.J., Buechler D., Rudlosky S. Performance evaluation of the lightning imaging sensor on the international space station. *Journal of Atmospheric and Oceanic Technology.* 2023, vol. 40, pp. 1063–1082. DOI: [10.1175/JTECH-D-22-0120.1](https://doi.org/10.1175/JTECH-D-22-0120.1).
- URL: <https://www.blitzortung.org/> (accessed December 12, 2024).
- URL: <https://www.eumetsat.int/features/animations-europes-first-lightning-imager> (accessed December 12, 2024).

URL: <https://meteoinfo.ru/mapsynop> (accessed December 12, 2024).

URL: <http://www.alwes.ru> (accessed December 12, 2024).

Original Russian version: Tkachev I.D., Vasilyev R.V., Zorkaltseva O.S., Poletaev A.S., Chensky A.G., Vasiliev K.M., Salimgoreev R.R., published in *Solnechno-zemnaya fizika*. 2025, vol. 11, no. 2, pp. 112–123. DOI: [10.12737/szf-112202510](https://doi.org/10.12737/szf-112202510). © 2025 INFRA-M Academic Publishing House (Nauchno-Izdatelskii Tsentr INFRA-M).

How to cite this article

Tkachev I.D., Vasilyev R.V., Zorkaltseva O.S., Poletaev A.S., Chensky A.G., Vasiliev K.M., Salimgoreev R.R. Experimental distributed network of VLF receivers for thunderstorm activity monitoring in the Baikal Natural Territory. *Sol.-Terr. Phys.* 2025, vol. 11, iss. 2, pp. 99–110. DOI: [10.12737/stp-112202510](https://doi.org/10.12737/stp-112202510).